

## APPENDIX A. ANALYSIS OF THE OPTIMALITY FOR THE PERSONALIZED-PRESERVING BENDERS DECOMPOSITION

Consider the following generalized formulation of the optimization problem for a decision maker in TES:

$$\min_{p_{d,t}, p_{m,t}} F(p_{d,t}, p_{m,t}) \quad (\text{A1})$$

$$\text{s.t. : } g_j(p_{d,t}, p_{m,t}) \leq 0 \quad \forall j = 1, 2, \dots, J \quad (\text{A2})$$

$$h_k(p_{d,t}, p_{m,t}) = 0 \quad \forall k = 1, 2, \dots, K \quad (\text{A3})$$

$$u_l(p_{d,t}, p_{m,t}) \leq 0 \quad \forall l = 1, 2, \dots, L \quad (\text{A4})$$

where  $(p_{d,t}, p_{m,t})$  represents the variables related to transactions,  $F(p_{d,t}, p_{m,t})$  represents the objective function of the decision maker, the inequality constraints  $g_j(p_{d,t}, p_{m,t})$  and equality constraints  $h_k(p_{d,t}, p_{m,t})$  are related to TES transactions. Additionally,  $u_l(p_{d,t}, p_{m,t})$  represents the safety constraints for the operation of the DN, which include sensitive topology information.

**Proposition 3.** *The relaxed problem (A1)-(A3) with Benders feasibility cuts as additional constraints are identical to the original optimization problem (A1)-(A4).*

*Proof.* To ensure that the topology information of the DN is not disclosed to TES participants, we first consider the relaxed optimization problem (A1)-(A3) without the safety constraints (A4), obtaining the optimal solution  $(p_{d,t}^*, p_{m,t}^*)$ . Next, TESO checks the PF in DN. If the safety constraints (A4) are not violated, then  $(p_{d,t}^*, p_{m,t}^*)$  is the final transaction. If the safety constraints (A4) are violated, we solve the following slack problem to determine violation  $E$ .

$$\min_{\epsilon_l} E = \sum_{l=1}^L \epsilon_l \quad (\text{A5})$$

$$\text{s.t. : } u_l(p_{d,t}, p_{m,t}) - \epsilon_l \leq 0, \quad 0 \leq \epsilon_l \quad \forall l = 1, 2, \dots, L \quad (\text{A6})$$

where  $\epsilon_l$  is the slack variable of the  $l$ -th safety constraint. When  $E^* \leq 0$ , it indicates that all safety constraints are not violated, and the corresponding solution  $(p_{d,t}^*, p_{m,t}^*)$  at this point is the optimal transactions to the original problem. If  $E^* > 0$ , it is necessary to regulate the transactions  $(p_{d,t}^*, p_{m,t}^*)$  so that  $E^* + \Delta E \leq 0$ . By performing a first-order Taylor expansion of  $E^*$  at point  $(p_{d,t}^*, p_{m,t}^*)$ , the relationship between  $(p_{d,t}^*, p_{m,t}^*)$  and  $\Delta E$  is obtained as follows:

$$\Delta E = \sum_{d \in \mathcal{D}} \sum_{l=1}^L \frac{\partial E}{\partial p_{d,t}} (p_{d,t} - p_{d,t}^*) + \sum_{l=1}^L \frac{\partial E}{\partial p_{m,t}} (p_{m,t} - p_{m,t}^*) \quad (\text{A7})$$

Next, by ensuring the following equation holds, we can achieve the optimal transaction that complies with the safety constraints.

$$E^* + \Delta E \leq 0 \quad (\text{A8})$$

However, the expression for  $E$  does not include  $(p_{d,t}^*, p_{m,t}^*)$ . To find the mathematical relationship between decision variables  $(p_{d,t}^*, p_{m,t}^*)$  and the constraint violation  $E$ , we need to formulate the dual of the slack problem shown as follows.

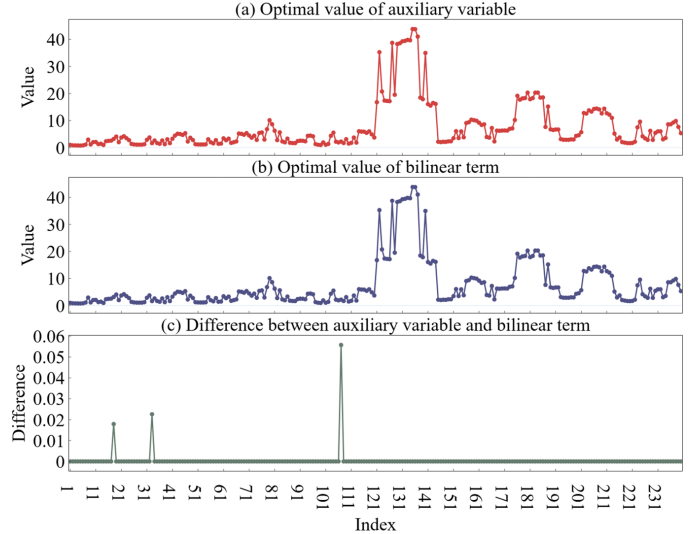


Fig. B1. Comparison between auxiliary variable and bilinear term

$$\max_{y_l} \Phi = \sum_{l=1}^L y_l \times u_l(p_{d,t}^{*'}, p_{m,t}^{*'}) \quad (\text{A9})$$

$$\text{s.t. : } 0 \leq y_l \leq 1 \quad \forall l = 1, 2, \dots, L \quad (\text{A10})$$

where  $y_l$  is the dual variable.

Since the slack problem is a linear programming problem, strong duality implies that  $\Phi^* = E^*$ , equation (A8) can be substituted as:

$$\Phi^* + \Delta \Phi \leq 0 \quad (\text{A11})$$

The Benders feasibility cut can be expressed as follows.

$$\Phi^* + \sum_{d \in \mathcal{D}} \sum_{l=1}^L \frac{\partial \Phi}{\partial p_{d,t}} (p_{d,t} - p_{d,t}^*) + \sum_{l=1}^L \frac{\partial \Phi}{\partial p_{m,t}} (p_{m,t} - p_{m,t}^*) \leq 0 \quad (\text{A12})$$

where  $\frac{\partial \Phi}{\partial p_{d,t}}$  and  $\frac{\partial \Phi}{\partial p_{m,t}}$  can be calculated according to (A9).

Continue adding Benders feasibility cuts as constraints to the relaxed problem (A1)-(A3) until  $E^* = \Phi^* = 0$ , which will yield the optimal solution. Since the Benders feasibility cuts (A12) are equivalent to the safety constraints (A4), the solution  $(p_{d,t}^*, p_{m,t}^*)$  obtained from the relaxed problem (A1)-(A3) with Benders feasibility cuts is also the optimal solution to the original problem (A1)-(A4).  $\square$

## APPENDIX B. MCCORMICK ENVELOPE FOR THE BILINEAR TERM IN RIMP

The bilinear term in RIMP is  $\tilde{p}_{c,t} \pi_{c,t}$  in the objective function (38). Following the McCormick envelope, we introduce auxiliary variables  $w_{c,t}$  to approximate  $\tilde{p}_{c,t} \pi_{c,t}$  and impose the following constraints for all  $c \in \mathcal{C}$  and  $t \in \mathcal{T}$ .

$$w_{c,t} \geq \underline{p}_{c,t} \pi_{c,t} + \tilde{p}_{c,t} \bar{\pi}_{c,t} - \bar{p}_{c,t} \underline{\pi}_{c,t} \quad (\text{B1})$$

$$w_{c,t} \geq \bar{p}_{c,t} \pi_{c,t} + \tilde{p}_{c,t} \bar{\pi}_{c,t} - \bar{p}_{c,t} \bar{\pi}_{c,t} \quad (\text{B2})$$

$$w_{c,t} \leq \bar{p}_{c,t} \pi_{c,t} + \tilde{p}_{c,t} \bar{\pi}_{c,t} - \bar{p}_{c,t} \underline{\pi}_{c,t} \quad (\text{B3})$$

$$w_{c,t} \leq \underline{p}_{c,t} \pi_{c,t} + \tilde{p}_{c,t} \bar{\pi}_{c,t} - \underline{p}_{c,t} \bar{\pi}_{c,t} \quad (\text{B4})$$

Therefore, the nonconvex bilinear term is approximated by linear term with linear constraints, and we can then compute the dual variables of the resulting linear programming.

In the McCormick envelope, the quality of the dual approximation depends directly on the tightness of the relaxation, namely how close the auxiliary variable  $w_{c,t}^*$  is to the true bilinear value  $\tilde{p}_{c,t}^* \pi_{c,t}^*$ . When  $w_{c,t}^*$  approaches  $\tilde{p}_{c,t}^* \pi_{c,t}^*$  closely, the linear envelope nearly coincides with the original nonconvex surface at the optimum. In this case, the local geometric properties of the relaxed problem, including marginal values and sensitivities of the constraints, align closely with those of the original problem. The resulting dual variables then can accurately reflect the true dual information of the original problem.

Fig. B1 illustrates the relationship between  $w_{c,t}^*$  and  $\tilde{p}_{c,t}^* \pi_{c,t}^*$  in RIMP, where Fig. B1(a) shows the optimal solution of  $w_{c,t}^*$ , Fig. B1(b) shows the optimal solution of  $\tilde{p}_{c,t}^* \pi_{c,t}^*$  and Fig. B1(c) shows their difference. At the optimum, the gap between  $w_{c,t}^*$  and  $\tilde{p}_{c,t}^* \pi_{c,t}^*$  is small, indicating that the linear envelope (B1)–(B4) closely matches the original surface at the optimum. The resulting dual variables therefore accurately reflect the true dual information of the original problem.

### APPENDIX C. FORMULATION OF BENDERS FEASIBILITY CUTS

The mathematical formulation of the Lindistflow model is as follows:

$$\mathbf{P}_{ij,t}^\phi + \sum_{d \in \mathcal{D}_j} \mathbf{p}_{j,d,t}^\phi = \sum_{c \in \mathcal{C}_j} \mathbf{p}_{j,c,t}^\phi + \sum_{k \in \mathcal{N}_j} \mathbf{P}_{j,k,t}^\phi \quad (\text{C1})$$

$$\mathbf{Q}_{ij,t}^\phi = \sum_{c \in \mathcal{C}_j} \mathbf{q}_{j,c,t}^\phi + \sum_{k \in \mathcal{N}_j} \mathbf{Q}_{j,k,t}^\phi \quad (\text{C2})$$

$$\|\mathbf{v}_{j,t}^\phi\|^2 = \|\mathbf{v}_{i,t}^\phi\|^2 - \mathbf{M}_{ij}^P \mathbf{P}_{ij,t}^\phi - \mathbf{M}_{ij}^Q \mathbf{Q}_{ij,t}^\phi \quad (\text{C3})$$

where  $\mathcal{D}_j$ ,  $\mathcal{C}_j$  and  $\mathcal{N}_j$  is the set of DERs, set of customers connected to node  $j$ , and set of nodes located downstream of node  $j$ , respectively. (C1), (C2) and (C3) are active power, reactive power flow equations and voltage balance equation, respectively. The matrices:

$$\mathbf{M}_{ij}^P = \begin{bmatrix} -2r_{ij}^{aa} & r_{ij}^{ab} - \sqrt{3}r_{ij}^{ab} & x_{ij}^{ac} + \sqrt{3}r_{ij}^{ac} \\ r_{ij}^{ba} + \sqrt{3}x_{ij}^{ba} & -2r_{ij}^{bb} & r_{ij}^{bc} - \sqrt{3}x_{ij}^{bc} \\ r_{ij}^{ca} - \sqrt{3}x_{ij}^{ca} & r_{ij}^{cb} + \sqrt{3}x_{ij}^{cb} & -2r_{ij}^{bb} \end{bmatrix}_{l_{ij}} \quad (\text{C4})$$

$$\mathbf{M}_{ij}^Q = \begin{bmatrix} -2x_{ij}^{aa} & x_{ij}^{ab} + \sqrt{3}r_{ij}^{ab} & x_{ij}^{ac} + \sqrt{3}r_{ij}^{ac} \\ x_{ij}^{ba} + \sqrt{3}r_{ij}^{ba} & -2x_{ij}^{bb} & x_{ij}^{bc} + \sqrt{3}r_{ij}^{bc} \\ x_{ij}^{ca} + \sqrt{3}r_{ij}^{ca} & x_{ij}^{cb} - \sqrt{3}r_{ij}^{cb} & -2x_{ij}^{cc} \end{bmatrix}_{l_{ij}} \quad (\text{C5})$$

According to equation (64), we refer to  $\frac{\partial \Theta}{\partial p_{d,t}}$  and  $\frac{\partial \Theta}{\partial p_{m,t}}$  as the simplex multipliers corresponding to  $p_{d,t}$  and  $p_{m,t}$ . The energy purchased from the MG is injected at the balancing node, like a special type of DER. Therefore, we only need to analyze  $\frac{\partial \Theta}{\partial p_{d,t}}$ . Assume that DER  $d$  is located at node  $j$  in phase  $\phi$ . In this case, we replace  $p_{d,t}$  with  $p_{j,d,t}^\phi$ , where the subscript  $j$  indicates its position in the DN. The mathematical expression of  $\frac{\partial \Theta}{\partial p_{j,d,t}^\phi}$  is as follows:

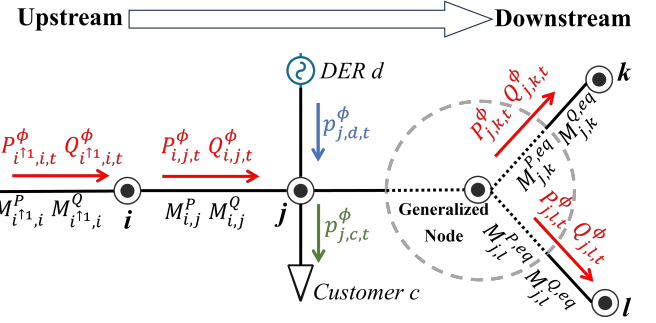


Fig. C1. Illustration of power flow between nodes

$$\frac{\partial \Theta}{\partial p_{j,d,t}^\phi} = \sum_{i,j \in \mathcal{I} \times \mathcal{T}} \{ (y_{i,t}^{V,\phi} - \bar{y}_{i,t}^{V,\phi}) \frac{\partial \|v_{i,t}^\phi\|^2}{\partial p_{j,d,t}^\phi} + (y_{ij,t}^{P,\phi} - \bar{y}_{ij,t}^{P,\phi}) \frac{\partial P_{ij,t}^\phi}{\partial p_{j,d,t}^\phi} + (y_{ij,t}^{Q,\phi} - \bar{y}_{ij,t}^{Q,\phi}) \frac{\partial Q_{ij,t}^\phi}{\partial p_{j,d,t}^\phi} \} \quad (\text{C6})$$

We need to calculate  $\frac{\partial \|v_{i,t}^\phi\|^2}{\partial p_{j,d,t}^\phi}$ ,  $\frac{\partial P_{ij,t}^\phi}{\partial p_{j,d,t}^\phi}$ , and  $\frac{\partial Q_{ij,t}^\phi}{\partial p_{j,d,t}^\phi}$ , which correspond to the voltage term, active power term, and reactive power term, respectively.

For clarity, we use  $i^{\uparrow n}$  to denote the  $n$ -th upstream node of node  $i$ , and  $i^{\downarrow n}$  to denote the  $n$ -th downstream node of node  $i$ . Fig. C1. illustrates the power flow between nodes. Node  $i$  is the upstream node of node  $j$ . Node  $j$  is upstream of nodes  $k$  and  $l$ . There are  $n$  intermediate nodes between node  $j$  and nodes  $k$  and  $l$ , which are treated as a generalized node. The power flow on the lines is marked in red. The power injected by DERs is marked in blue. The power consumed by customers is marked in green. The impedance matrix of the transmission lines is shown in black. Since the structure of the distribution network is radial, we define the active power distribution coefficients  $\alpha_k^\phi$  and  $\alpha_l^\phi$ . They satisfy the following relationships.

$$\alpha_k^\phi + \alpha_l^\phi = 1, \quad \frac{\alpha_k^\phi}{\alpha_l^\phi} = \frac{P_{jk,t}^\phi}{P_{jl,t}^\phi} \quad (\text{C7})$$

A detailed analysis of the calculation of these three terms is provided below. By substituting the following results into equation (64), the Benders feasibility cuts can be obtained.

#### A. Calculation of the voltage term:

Due to the presence of mutual inductance, the injected power from DER affects the three-phase voltages at nodes in the DN. Therefore, in this section, we use  $\phi_1$  to denote the phase of the voltage and  $\phi_2$  to denote the phase of the DER injected power. The calculation of  $\frac{\partial \|v_{j,t}^{\phi_1}\|^2}{\partial p_{j,d,t}^\phi}$  can be divided into the following cases.

1)  $i=j$ :

As shown in Fig. C1, when  $i=j$ , we calculate the impact of the injected DER power at node  $j$  on its own voltage. According to equations (C1) and (C3), we can obtain:

$$\frac{\partial \|v_{j,t}^{\phi_1}\|^2}{\partial p_{j,d,t}^\phi} = -\mathbf{M}_{j^{\uparrow 1}j}^P[\phi_2, \phi_1] = -\mathbf{M}_{ij}^P[\phi_2, \phi_1] \quad (\text{C8})$$

where  $\mathbf{M}_{j^{\uparrow 1}j}^P[\phi_2, \phi_1]$  represents the corresponding element in matrix  $\mathbf{M}_{j^{\uparrow 1}j}^P$ . For example, if  $\phi_1=\phi_2=a$ , then  $\mathbf{M}_{j^{\uparrow 1}j}^P[a, a] =$

$$\begin{aligned} & -2r_{j \uparrow 1}^{aa} \\ 2) & i \in j^{\uparrow n}: \end{aligned}$$

When  $i$  is a downstream node of  $j$ , we denote  $i$  as  $k$  for consistency with Fig. C1. And there are  $n$  intermediate nodes between  $j$  and  $k$ . Here, the distribution coefficients of active power flow  $\alpha_k^\phi$  and  $\alpha_l^\phi$  are introduced. Similarly, based on equations (C1) and (C3), as well as the coupling relationship between nodes, we can obtain:

$$\frac{\partial \|v_{k,t}^{\phi 1}\|^2}{\partial p_{j,d,t}^{\phi 2}} = -\mathbf{M}_{j \uparrow 1,j}^P[\phi 2, \phi 1] + \alpha_k^\phi \mathbf{M}_{jk}^{P,eq}[\phi 2, \phi 1] \quad (\text{C9})$$

where  $\mathbf{M}_{jk}^{P,eq}[\phi 2, \phi 1]$  is the equivalent impedance matrix between node  $j$  and node  $k$ .

$$3) i \in j^{\uparrow n}:$$

When  $i$  is an upstream node of  $j$ , and there are  $n$  intermediate nodes between  $i$  and  $j$ . Since the structure of DN is radial, there is no other injected power upstream of node  $j$ . Similarly, with equations (C1) and (C3), the voltage term can be calculated as follows.

$$\frac{\partial \|v_{i,t}^{\phi 1}\|^2}{\partial p_{j,d,t}^{\phi 2}} = -\mathbf{M}_{i \uparrow 1,i}^P[\phi 2, \phi 1] \quad (\text{C10})$$

#### 4) $i$ is the connection point with MG:

When node  $i$  serves as the connection point to the MG, whose voltage is fixed and is not affected by the DERs in the DN. Therefore, we can derive:

$$\frac{\partial \|v_{i,t}^{\phi 1}\|^2}{\partial p_{j,d,t}^{\phi 2}} = 0 \quad (\text{C11})$$

### B. Calculation of the active power term:

According to the Lindisflow model, PF distribution in different phases do not affect each other. Therefore, we only consider the impact of DER injected power on the PF distribution of the same phase. The calculation of active power term can be divided into the following cases.

#### 1) Line located downstream of node $j$ :

When the line is located downstream of node  $j$ , as shown in Fig. C1, we take  $\frac{\partial P_{jk,t}^\phi}{\partial p_{j,d,t}^\phi}$  as an example. According to equation (C1), we can calculate:

$$\frac{\partial P_{jk,t}^\phi}{\partial p_{j,d,t}^\phi} = \alpha_k^\phi \quad (\text{C12})$$

#### 2) Line located upstream of node $j$ :

When the line is located upstream of node  $j$ , we take  $\frac{\partial P_{ij,t}^\phi}{\partial p_{j,d,t}^\phi}$  as an example. According to equation (C1), we can calculate:

$$\frac{\partial P_{ij,t}^\phi}{\partial p_{j,d,t}^\phi} = -1 + \sum_{k \in \mathcal{N}_j} \alpha_k^\phi \quad (\text{C13})$$

If there exist downstream nodes connected to node  $j$ ,  $\sum_{k \in \mathcal{N}_j} \alpha_k^\phi = 1$ , so  $\frac{\partial P_{ij,t}^\phi}{\partial p_{j,d,t}^\phi} = 0$ . If there is no downstream nodes connected to node  $j$ , then  $\frac{\partial P_{ij,t}^\phi}{\partial p_{j,d,t}^\phi} = -1$ .

### C. Calculation of the reactive power term:

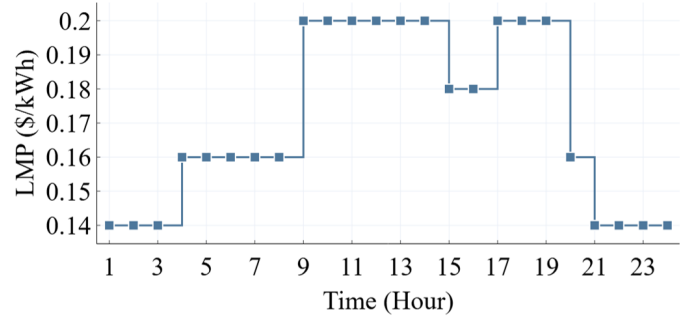


Fig. D1. LMP in the case study

TABLE D1  
PARAMETERS OF DERs AND MAIN GRID

Parameter	Value	Parameter	Value
$p_{g1,t}$ (kW)	0	$\bar{p}_{g2,t}$ (kW)	125
$p_{g2,t}$ (kW)	0	$\bar{p}_{g2,t}$ (kW)	100
$p_{WT,t}$ (kW)	0	$\bar{p}_{WT,t}$ (kW)	Available power
$p_{PV,t}$ (kW)	0	$\bar{p}_{PV,t}$ (kW)	Available power
$p_m$ (kW)	0	$\bar{p}_m,t$ (kW)	200
$\gamma_{g1,t}$ (\$/kWh)	0.075	$\gamma_{g2,t}$ (\$/kWh)	0.05
$\gamma_{WT,t}$ (\$/kWh)	0	$\gamma_{PV,t}$ (\$/kWh)	0
$\pi_{d,t}$ (\$/kWh)	0	$\bar{\pi}_{d,t}$ (\$/kWh)	$\max(0.16, \text{LMP}_t)$

In our study, the DERs only output active power and their reactive power is not considered, the active power output from the DERs does not affect the reactive power distribution in the DN. Based on this, we can draw the following equation.

$$\frac{\partial Q_{ij,t}^\phi}{\partial p_{j,d,t}^\phi} = 0 \quad (\text{C14})$$

### APPENDIX D. PARAMETER SETTINGS IN CASE STUDY

#### A. Parameters of DERs and main grid

Since DERs are small-capacity generation units, the maximum output power for G1 and G2 is set to 125 kW and 100 kW, respectively. For WT and PV, their maximum output power at time slot  $t$  is their maximum available power, and their minimum output power is 0. The energy purchased from the MG is limited by the transformer capacity, with the maximum power set to 250 kW. The generation costs for G1 and G2 are set to 0.075 \$/kWh and 0.05 \$/kWh, respectively, while the generation costs for WT and PV are set to 0. The energy selling price of DERs at time slot  $t$  is bounded below by 0 and above by  $\max(0.16, \text{LMP}_t)$ , where  $\text{LMP}_t$  denotes the LMP at time slot  $t$ . This bound prevents the DER manager from setting excessively high energy selling prices. The values of parameters related to DERs and MG are shown in Table D1. The LMP is shown as Fig. D1.

#### B. Parameters of customers

Different types of customers have varying abilities to adjust their load profiles during PBDR. RL are more flexible with their electricity use, allowing their power consumption in each time slot to be adjusted 10% of the original amount. In contrast, the adjustment limits for IL, CL, and AL are 5% of their original power consumption. The LA sets the bounds for personalized electricity prices for customers at 0.12 \$/kWh and 0.24 \$/kWh, corresponding to peak and off-peak rates. The total electricity

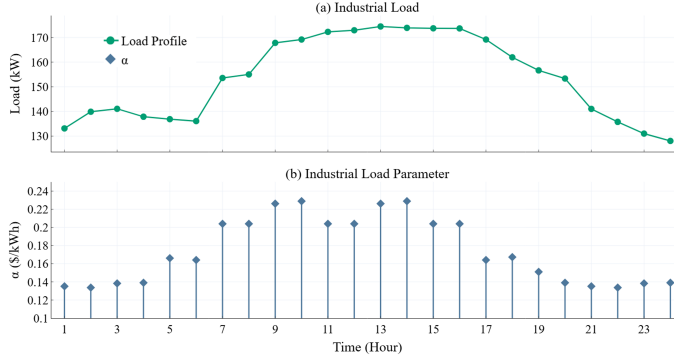


Fig. D2. Illustration of the load profile and utility parameter

TABLE D2  
PARAMETERS OF CUSTOMERS

Parameter	Value	Parameter	Value
$\underline{p}_{c,t}^{RL}$ (kW)	$0.9p_{c,t}^{RL,ori}$	$\bar{p}_{c,t}^{RL}$ (kW)	$1.1p_{c,t}^{RL,ori}$
$\underline{p}_{c,t}^{IL}$ (kW)	$0.95p_{c,t}^{IL,ori}$	$\bar{p}_{c,t}^{IL}$ (kW)	$1.05p_{c,t}^{IL,ori}$
$\underline{p}_{c,t}^{CL}$ (kW)	$0.95p_{c,t}^{CL,ori}$	$\bar{p}_{c,t}^{CL}$ (kW)	$1.05p_{c,t}^{CL,ori}$
$\underline{p}_{c,t}^{AL}$ (kW)	$0.95p_{c,t}^{AL,ori}$	$\bar{p}_{c,t}^{AL}$ (kW)	$1.05p_{c,t}^{AL,ori}$
$\pi_{c,t}$ (\$/kWh)	0.12	$\bar{\pi}_{c,t}$ (\$/kWh)	0.24
$\Pi_{c,t}$ (\$/kWh)	4.32		

price over 24 hours must not exceed 4.32 \$, reflecting 12 peak

and 12 off-peak time slots. The values of parameters related to customers are shown in Table D2. Additionally, the parameter  $\alpha_{c,t}$  in the customer utility function varies over time. Since  $\alpha_{c,t}$  represents the income that customer  $c$  obtains from consuming 1 kWh of electricity at time slot  $t$ , we set the fluctuations of  $\alpha_{c,t}$  to resemble the original load profile. Taking the industrial customer at node 7 as an example, Fig. D2 illustrates both its load profile and the corresponding values of  $\alpha_{c,t}$ .

### C. Parameters of DN

In the DN, the base value for power is set to 1000 kVA, and the base value for voltage is set to 220 V. In our study, The maximum transmitted active and reactive power over the cable are set to 0.5 p.u. and 0.4 p.u., respectively. The voltage limits at the nodes are set between 0.95 p.u. and 1.05 p.u. The tap position of the transformer connected to the MG is set to 0, so the voltage at node 2 is 1 p.u. The values of parameters related to DN are shown in Table D3.

TABLE D3  
PARAMETERS OF DISTRIBUTION NETWORK

Parameter	Value	Parameter	Value
$\underline{P}_{i,j,t}^\phi$	-0.5	$\bar{P}_{i,j,t}^\phi$	0.5
$\underline{Q}_{i,j,t}^\phi$	-0.4	$\bar{Q}_{i,j,t}^\phi$	0.4
$\underline{v}_{i,t}^\phi$	0.95	$\bar{v}_{i,t}^\phi$	1.05